

New Synthetic Models of Cytochrome P450: How Different Are They from the Natural Species?

Sebastian Kozuch,^a Tycho Leifels,^b Dominik Meyer,^b Laura Sbaragli,^b Sason Shaik,^{*a} Wolf-D. Woggon^{*b}

^a Department of Organic Chemistry and The Lise Meitner-Minerva Center for Computational Quantum Chemistry, Givat Ram Campus, Jerusalem 91904, Israel

^b Department of Chemistry, University of Basel, St. Johannis-Ring 19, 4056 Basel, Switzerland
Fax +41(61)2671102; E-mail: wolf-d.woggon@unibas.ch

Received 3 December 2004

Abstract: Soluble and matrix-bound P450 enzyme models have been synthesized carrying a SO_3^- ligand coordinating to iron. These complexes display features very similar to cofactors of enzymes such as P450_{cam} with respect to electrochemistry and UV/Vis spectroscopy. Further they catalyze epoxidation reactions with turnover numbers up to 1800. DFT calculations revealed that the coordination of SO_3^- to Fe(III) produces an active species that displays allylic hydroxylation and epoxidation reactivity patterns that are nearly indistinguishable from those calculated for the natural active species of the enzyme cytochrome P450.

Key words: catalysis, enzyme models, DFT calculations, heme-thiolate proteins, iron porphyrins

Cytochromes P450 are naturally abundant heme-thiolate proteins that catalyze a broad spectrum of stereoselective oxidation reactions through reductive cleavage of molecular oxygen bound to iron and 'insertion' of a single oxygen atom into activated or non-activated positions of the substrate.¹ Accordingly, these enzymes are the prototype of a monooxygenase system. The significance of these proteins derives from their participation in the metabolism of endogenous compounds and xenobiotics, e.g. in human glands highly substrate specific P450s catalyze the formation of steroid hormones from cholesterol, whereas in hu-

man liver P450s exhibit a rather broad substrate tolerance hydroxylating drugs and other xenobiotics and rendering them into easily excretable compounds.

Ever since these enzymes were first identified by the shift of the Soret band from ca. 410 nm [$\text{Fe(III)}\cdot\text{S}^-$ resting state] to ca. 450 nm [$\text{OC}\cdot\text{Fe(II)}\cdot\text{S}^-$]² the significance of the unique thiolate ligand has been debated. In this context the investigation of synthetic active site analogues provided interesting clues.³ The bridged $\text{Fe(III)}\cdot\text{S}^-$ porphyrins **1–3** (Figure 1)⁴ are resting state models not only with respect to spectroscopy but also concerning reactivity, since for **1** it was possible indeed to demonstrate the intramolecular hydroxylation of a non-activated position in the alkane bridge spanning the distal side of the porphyrin.⁵

Interestingly, however, the redoxpotentials of **1–3**⁶ were shown to be far more negative than the resting state of P450_{cam} ($E_0 = -290$ mV)⁷ a cytosolic crystallizable protein from *Pseudomonas putida*. From these results it was concluded that the charge at the thiolate ligand of P450_{cam} is somewhat 'shielded'. In fact this was shown to be true using a refined X-ray structure of P450_{cam} ⁸ revealing H-bonding of several amino acids of the protein backbone to the thiolate (Figure 2).

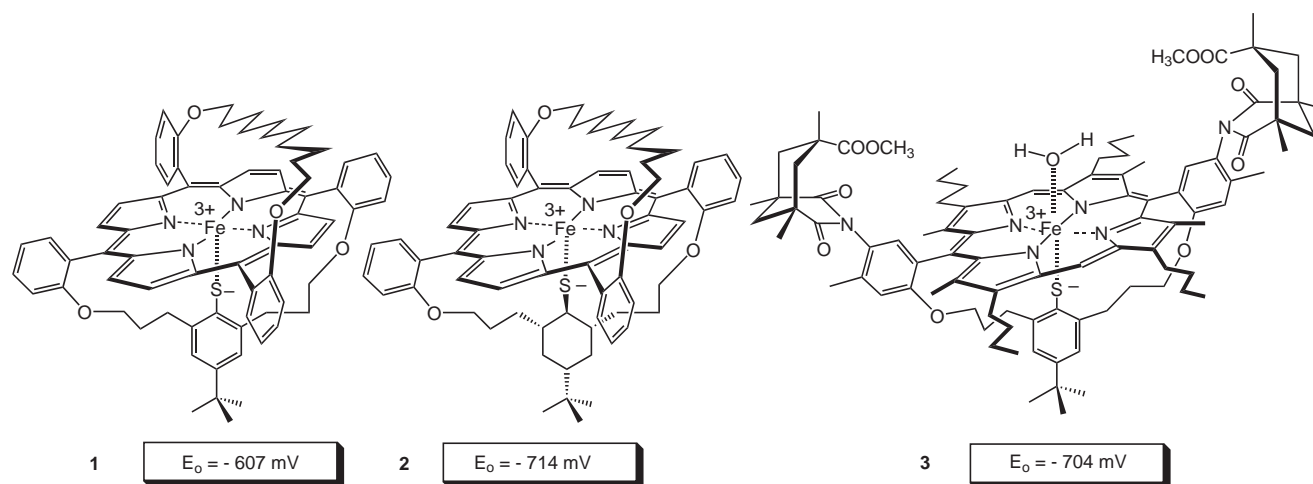


Figure 1 Enzyme models of the resting state of cytochrome P450.

SYNLETT 2005, No. 4, pp 0675–0684

Advanced online publication: 22.02.2005

DOI: 10.1055/s-2005-863724; Art ID: Y04604ST

© Georg Thieme Verlag Stuttgart · New York

Subsequently, model compounds **4** and **5** were reported mimicking this situation, confirming the idea that indeed the redoxpotential of P450_{cam} is largely dependent on the charge density at the thiolate coordinating to iron. Due to the non-covalent attachment of the fifth ligand complexes **4** and **5** are very elegant models for analytical purposes but are not suitable for catalytic reactions.⁹

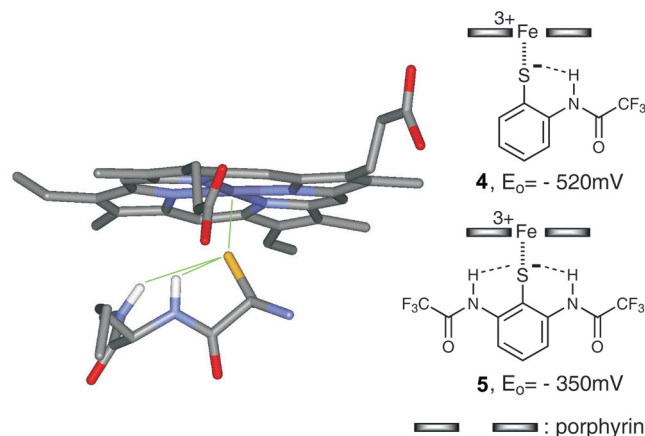


Figure 2 H-bonding of the thiolate ligand of P450_{cam} and corresponding model compounds **4** and **5**, which mimic the proximal coordination site.

To find more suitable models, we sought for an alternative species that would be synthetically convenient and theoretically appropriate, i.e. to replace the thiolate ligand for SO₃⁻. In this case the charge donating character of the ligand should be reduced to an extent similar to -H·S·H- and one could predict a considerable anodic shift of E₀ and further an increase in stability of the model complex in the presence of strong co-oxidants. In this communication we wish to report the preparation of suitable compounds comparing characteristic features of these new complexes with earlier Fe(III)·S⁻ enzyme models and present DFT calculations that at least in part support the synthetic concept.

Synthesis of Iron Porphyrins

It is known that electron-withdrawing groups in the periphery of the porphyrin shift the redox potential of the central metal towards more positive values. Thus, we decided to attach Cl to phenyl groups linked to the *meso*-position of the macrocycle and prepared target compound **6** according to Scheme 1. The starting material dipyrromethane **7** and the protected aldehyde **8** were prepared following standard procedures.⁴ The resulting porphyrin **9** was deprotected and the free phenol **10** obtained as a mixture of atropisomers α,α -**10** and α,β -**10** that are interconvertible at room temperature. The mixture of atropisomers **10** was then condensed under diluted conditions with the dimesylate **11**, which has been prepared according to our own protocol.⁴ The product **12** was treated with strong base to give the mono-bridged free-base porphyrin **13**

ready for iron insertion. Treatment of **13** with FeBr₂ yielded **14**, which on exposure to oxygen furnished **6** carrying a SO₃⁻ ligand coordinating to iron. According to EPR spectroscopy enzyme models **6** and **14** are both high-spin complexes with *g*-values of 5.76 and 7.45, 4.50, 3.40 respectively. They display distinct UV/Vis spectra with $\lambda_{\max} = 422$ nm (**14**) and $\lambda_{\max} = 414$ nm (**6**).

Cyclic voltammetry of complexes **14** and **6** revealed reversible redox behavior attributed to Fe(III)/Fe(II), see Figure 3, from which characteristic E₀ were calculated. In comparison to complexes **1–3** it is obvious that the addition of electron-withdrawing groups in the *meso*-phenyl rings causes an anodic shift of E₀ = 140–250 mV. The increment resulting from an exchange of thiolate coordination (**14**) for the SO₃⁻ ligand (**6**) is +280 mV.

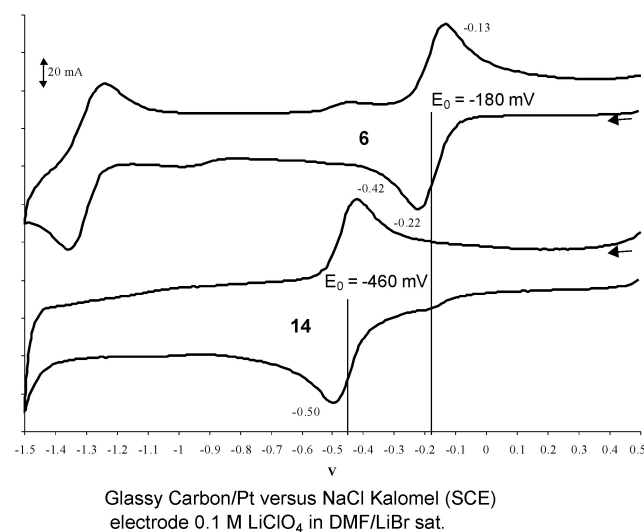
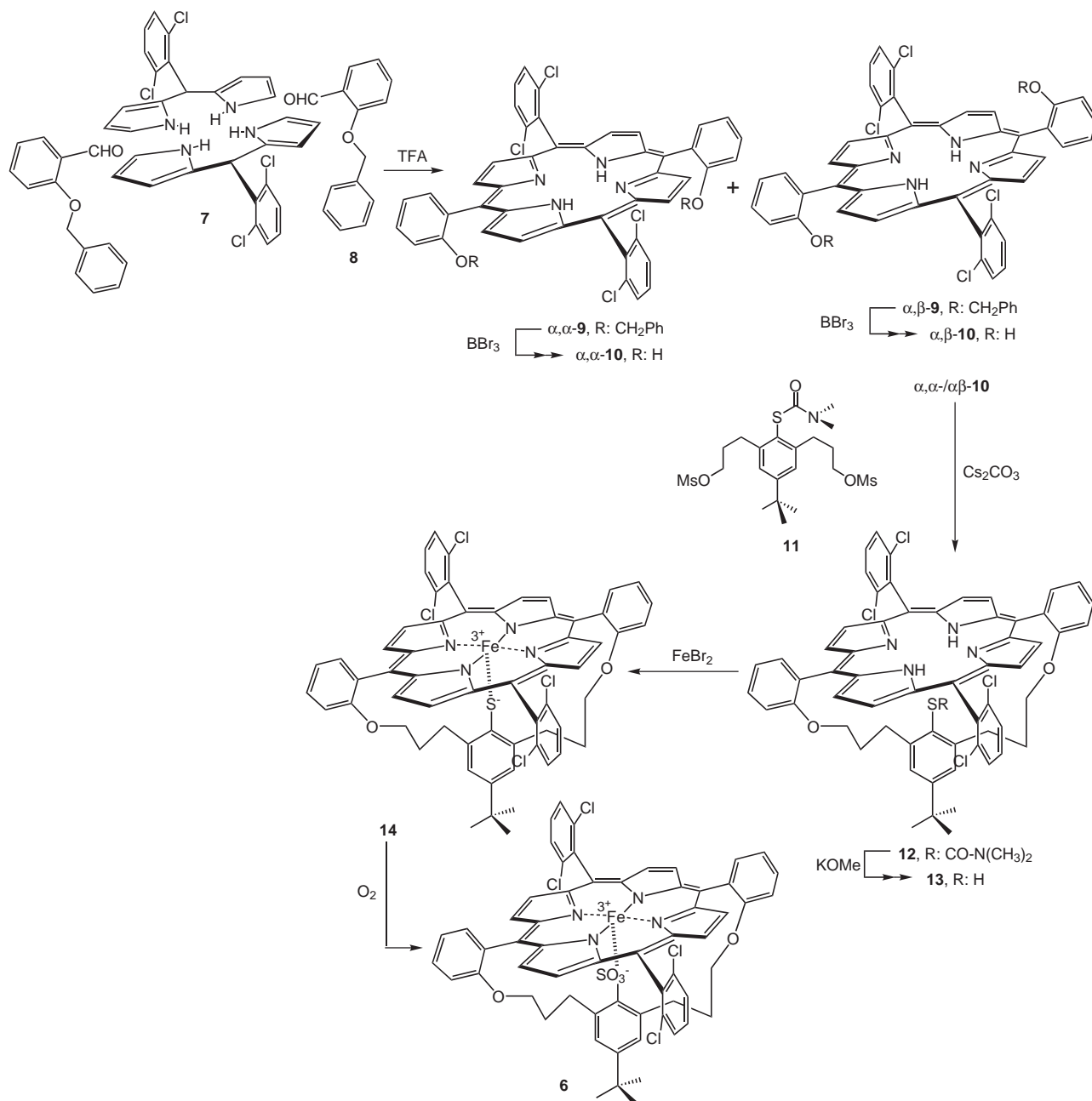


Figure 3 Cyclic voltammograms of **6** (trace above) and **14** (trace below); glassy carbon/Pt vs. SCE, 0.1 M LiClO₄ in LiBr sat. DMF.

Accordingly, complex **6** exhibits a redoxpotential identical to E₀ of the E·S complex of P450_{cam}. Further the SO₃⁻ ligand (**6**) has a considerable practical advantage over thiolate coordination (**14**) concerning catalytic reactions. In this context it is important to note that despite considerable steric congestion at the thiolate ligand in complexes **1–3** and **14** oxidants used for the ‘shunt pathway’ such as PhIO, PhF₃IO, and H₂O₂ and in particular O₂ oxidize the thiolate slowly via -SO⁻, -SO₂⁻ to SO₃⁻ creating an undesired mixture of oxidants during reactions. For **6** having a stable coordination site it is even possible to work outside the glove box.

To compare homogenous reactions of catalyst **6** with heterogeneous conditions we prepared the polymer bound porphyrin **15** according to Scheme 2. The aldehyde **16** was condensed with the dipyrromethane **7** to yield the porphyrin **17** as mixture of α,α - and α,β -atropisomers. BBr₃ treatment liberated the phenolic OH groups ready for macrocyclization with the dimesylate **11**. The mono-bridged porphyrin **19** was deprotected at sulfur and at the peripheric esters to furnish the free base porphyrin diacid



Scheme 1 Synthesis of the P450 enzyme mimic **6** carrying a SO_3^- ligand coordinating to iron.

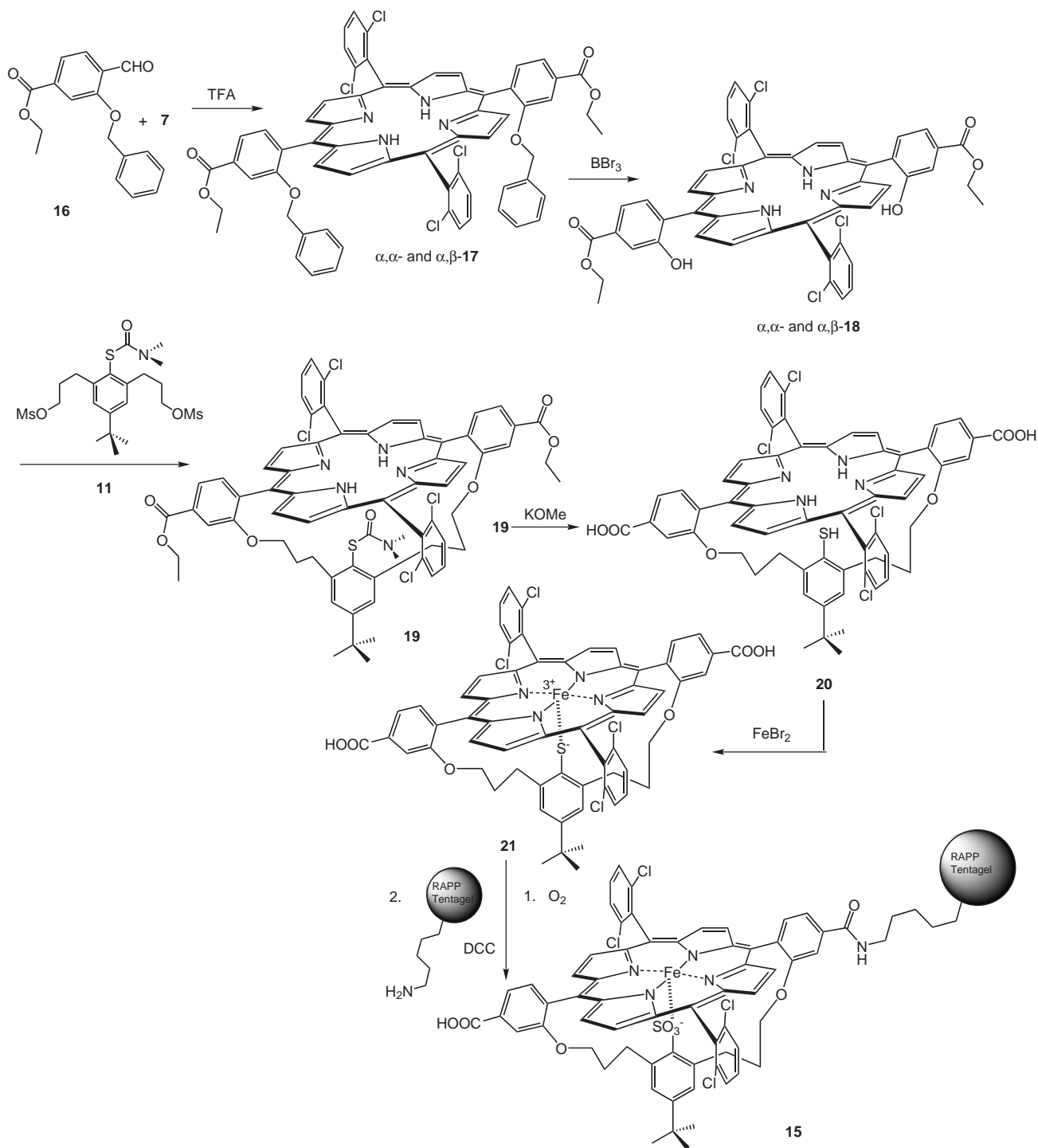
20. Iron insertion gave **21** and subsequent oxidation yielded the desired iron(III) complex carrying a SO_3^- ligand. Activation of the acid and coupling to the amino groups of RAPP Tentagel finally gave the immobilized catalyst **15**. The epitopic density of **15** was determined by UV (420 nm) 20 mmol porphyrin/g Tentagel which was confirmed by a Ninhydrin test after acetylation of the residual amino groups at the polymer and subsequent derivatization of the free COOH groups at **15**.

Catalytic reactions were pursued under standardized conditions with substrates such as **22–25** using PhIO as the 'O'-source. Some results are shown in Scheme 3 demonstrating the capability of **6** and **15** to catalyze epoxidations even in a regioselective fashion. In general turnovers

achieved with **6** and **15** exceed those obtained with model compounds **1–3**, **14** by a factor of ca. 50. Hence, these experiments demonstrate that iron porphyrins carrying a SO_3^- ligand are valuable P450 mimics with respect to electrochemistry and reactivity.

Results of Theoretical Modeling

The iron-oxo porphyrin species **6_{Ph}** and **6_{Me}**, which serve as models for **6**, are shown in Figure 4 in two different coordination modes, one with an Fe-O bond between the heme and the RSO_3^- ligand [**6_{Ph}(A)** and **6_{Me}(A)**], and the other with an Fe-S bond [**6_{Ph}(B)** and **6_{Me}(B)**]. It is apparent



Scheme 2 Synthesis of the polymer-bound P450 mimic.

that the second option (mode **B**) is highly unfavorable, the Fe-S bond being too long and the species laying 19–31 kcal/mol higher than the one with the Fe-O bond (mode **A**). In addition, frequency calculations show that $6_{Ph}(\mathbf{B})$ and $6_{Me}(\mathbf{B})$ are not really stable minima but are saddle points for the exchange of the three different Fe-O bonds. Thus the synthetic model involves an iron coordinated to an oxygen, compared with the natural enzyme, which possesses an Fe-S bond. The species $6_{Ph}(\mathbf{A})$ and $6_{Me}(\mathbf{A})$

have two low lying states, a high-spin (HS) quartet and a low-spin (LS) doublet. The energy differences are rather small, 0.16–0.31 kcal/mol, and the closely lying HS-LS pair of states is much like the situation in the analogous species in the P450 enzyme,¹⁰ known also as Compound I (Cpd I). Thus, the synthetic model resembles in this sense the natural species, and moreover, $6_{Me}(\mathbf{A})$ is a faithful model of $6_{Ph}(\mathbf{A})$, and hence can replace the latter in the subsequent reactivity calculations.

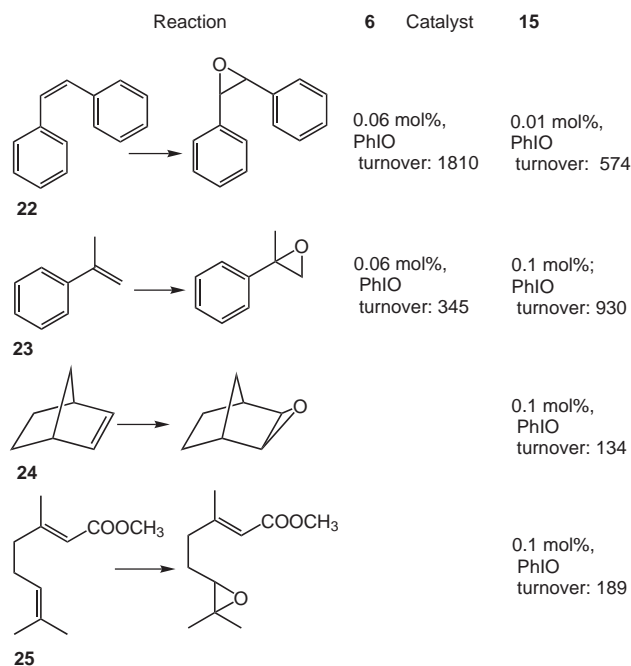
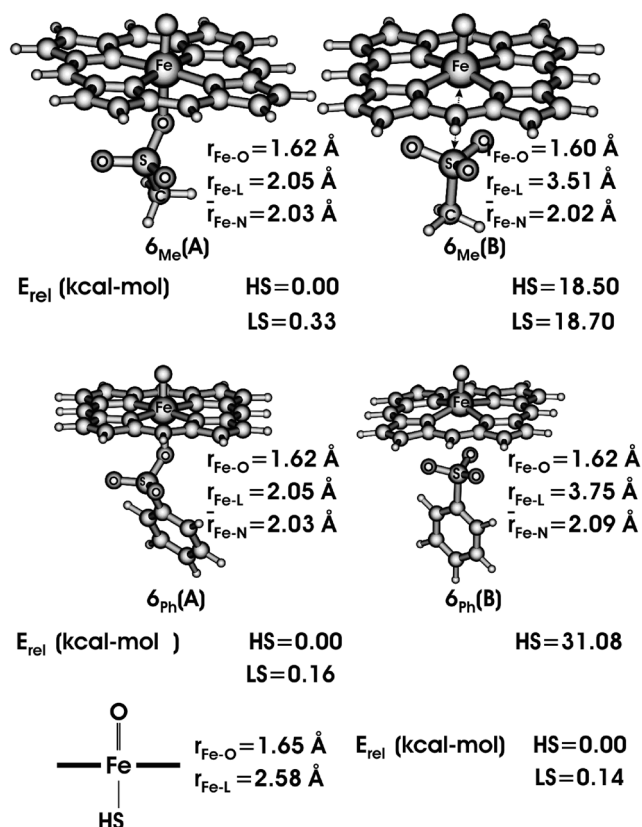
Scheme 3 Catalytic epoxidations with P450 mimics **6** and **15**.

Figure 4 Structures of the iron-oxo porphyrin complexes [optimized with LACVP+*(Fe)6-31+G*(C,H,N,O)], δ_{Ph} and δ_{Me} , of heme with RSO_3^- (R = Ph, Me) in the coordination modes A and B. Energy data underneath the structures show the relative energies of the low-spin state complexes in kcal/mol. Shown is the corresponding P450 species, too.¹⁰ Note that each complex possesses high-spin (HS) and varieties. Data obtained in LACVP+* basis set.

Figure 5 shows the spin-density distribution of the HS states of $\delta_{\text{Ph}}(\text{A})$ and $\delta_{\text{Me}}(\text{A})$. It is apparent that the species are both tri-radicaloids, with three unpaired electrons residing in π^* -orbitals and in a porphyrin centered orbital called a_{2u} (the a_{2u} orbital, as shown in the orbital diagram, depicted in the figure alongside the spin density diagrams. The LS states show analogous distribution, with the exception that the spin state of the a_{2u} electron is now coupled antiferromagnetically to the triplet pair in the π^*_{xz} - and π^*_{yz} -orbitals. In terms of electronic structure there is difference between the model species and the species of P450, where the a_{2u} electron is highly delocalized over the sulfur in a manner that is very sensitive to the polarity and hydrogen bonding capability of the environment.¹¹

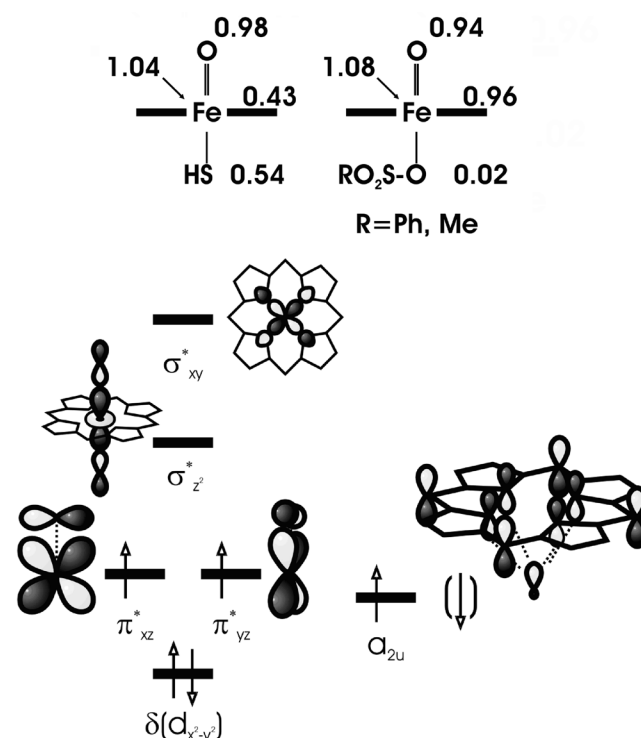


Figure 5 Spin density distribution in the HS states of the stable complexes $\delta_{\text{Ph}}(\text{A})$ and $\delta_{\text{Me}}(\text{A})$ and in the corresponding P450 model **6**. Alongside the structures we show a schematic orbital diagram of the key orbitals.

In summary, we may safely conclude that the synthetic reagent contains in fact an Fe-O bond, unlike the natural system that contains an Fe-S bond. Furthermore, the model system has a pure porphyrin radical-cationic situation, as opposed to the natural system, which is a mixed sulfur-porphyrin radical species. On the other hand, much as the iron-oxo species of the natural system, here too, the active species of the synthetic model is a two-state oxidant and will be expected to exhibit two-state reactivity (TSR).¹² With the above differences and similarities between the two iron-oxo species of the synthetic model, it would be interesting to compare the reactivity of the synthetic model $\delta_{\text{Me}}(\text{A})$ with that of the P450 Cpd I model.

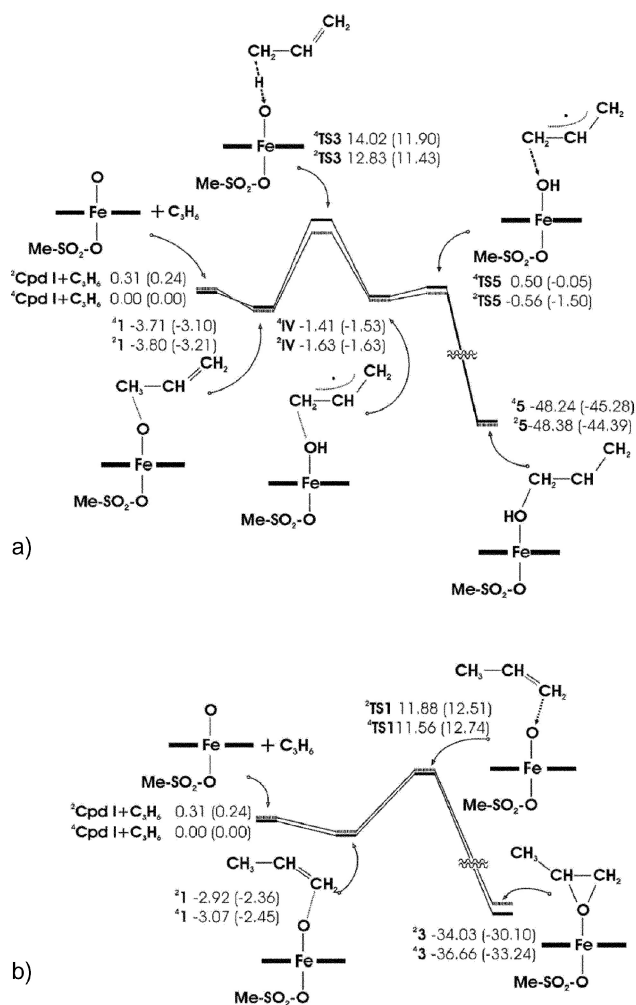


Figure 6 High-spin (HS) and low-spin (LS) energy profiles for the reaction of $6_{Me}(A)$ with propene, (a) C-H hydroxylation, and (b) C=C epoxidation. All energies are given in kcal/mol relative to the LS reactants. The energy data in parentheses include zero point energy correction. All calculations were done with the LACVP basis set.

Reactivity Patterns of the Active Species

The reaction of Cpd I with propene has been studied extensively in the past,¹⁰ and this will allow us to compare the reactivity patterns of a P450 species with those of $6_{Me}(A)$. The reaction profile for allylic hydroxylation of propene by $6_{Me}(A)$ depicted in Figure 6 (a) shows the commonly encountered bi-phasic pathway, with a bond activation phase followed by radical rebound.¹³ The doubling of the profile corresponds to TSR that arises from the HS and LS states of the iron-oxo active species.¹³ As before, here too, the HS mechanism is truly stepwise with a significant barrier for rebound, while the LS profile is effectively concerted with a negligible barrier (0.1 kcal/mol) for rebound. Figure 6 (b) shows the corresponding TSR profiles for epoxidation, and here both HS and LS pathways are effectively concerted; no intermediates could be detected. The experimental results, indeed, show only stereospecific epoxidations, see Scheme 3.

To project the similarities and differences between the reactivity of the synthetic model and the natural P450 species, Figure 7 shows a superimposition of the two profiles, using color-coding. There are some minor differences between the two profiles; the most notable difference is the rebound step, which exhibits higher rebound barriers for the native P450; this feature has been addressed in a recent review article, where a valence bond model for the rebound was used to rationalize trends in the rebound barriers.¹³ This means in turn that the synthetic model should be a slightly more stereoselective reagent compared to the natural species. In addition, the synthetic model shows a small preference for C-H hydroxylation over C=C epoxidation, while the natural species has an opposite slight preference. Other than these differences, the reaction profiles show almost a perfect superimposition that discloses the fundamental similarity between the two reagents.

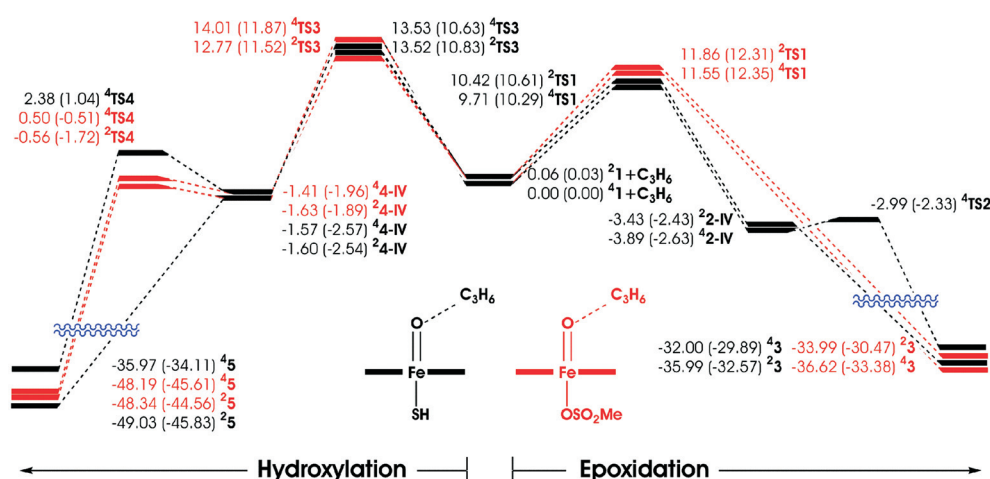


Figure 7 Color-coded and superimposed high-spin (HS) and low-spin (LS) energy profiles for the reaction of $6_{Me}(A)$ (red) and of Cpd I (black) with propene. The reactants are placed in the mid-diagram. The energies (in kcal/mol) are given relative to the separated reactants.

In summary, comparison of experimental data to theoretical calculations shows that the action of P450 enzymes can be mimicked by synthetic iron porphyrins designed to control the redox potential and reactivity by electron withdrawing subunits at the porphyrin's periphery and through changing the thiolate coordination for a SO_3^- ligand to iron.

Theoretical Methods

The calculations were performed with the hybrid functional, B3LYP[Ref], using the basis set combination LACVP⁶⁺(Fe)6-31G⁶⁺(H,C,N,O) and LACVP(Fe)6-31G(H,C,N,O), both of them giving virtually the same geometric and electronic characteristics, as reported in previous calculations of the Jerusalem group.¹³ Initially, we calculated the iron-oxo porphyrin species **6_{Ph}** including the phenyl group. Subsequently, we tested a smaller model system, with methyl replacing phenyl, and labeled as **6_{Me}**. A few different states were calculated to ascertain the nature of the ground state for both species. The paper describes only the ground states, while the rest of the data are relegated to the supplementary material. Since **6_{Ph}** and **6_{Me}** were found to be very similar, the reaction profiles were studied with **6_{Me}**, using propene as a substrate that can undergo both C-H hydroxylation and C=C epoxidation.¹³ The results with the iron-oxo porphyrin species of P450 were taken from a previous computational work.¹⁰ All critical species (intermediates, transition states) were ascertained by frequency calculation. The programs JAGUAR 4.2¹⁴ and GAUSSIAN 98¹⁵ were used throughout; the former is faster in geometry optimization, the latter is more efficient and accurate in frequency calculations.

2-Benzyloxy-benzaldehyde (8)

Salicylaldehyde (11.00 g, 90.0 mmol), (18.80 g, 103 mmol) potassium carbonate and (17.04 g, 99.6 mmol) benzyl bromide were dissolved in 400 mL MeOH and heated under reflux for 4 h. The residue was filtered off, the filtrate taken up in CH_2Cl_2 and washed with 1 N HCl. The water phase was extracted three times with CH_2Cl_2 , the combined organic phases were partially reduced at the rotavapor and washed with brine, dried over Na_2SO_4 and evaporated. The residue was chromatographed on silica (CH_2Cl_2 -hexane, 1:1) and recrystallized in MeOH-hexane to obtain 9.93 g (46.8 mmol, 52%) of **8** as colorless needles; mp 46–47 °C. $R_f = 0.22$ (silica, CH_2Cl_2 -hexane, 1:1).

¹H NMR (300 MHz, CDCl_3): $\delta = 10.55$ (s, 1 H, CHO), 7.86–6.99 (m, 9 H, aryl), 5.17 (s, 2 H, benzyl).

¹³C NMR (75 MHz, CDCl_3): $\delta = 189.8, 160.5, 136.2, 136.0, 128.5-127.4$ (6 C), 125.3, 121.1, 113.1, 70.5.

UV/Vis (CH_2Cl_2): λ_{max} (%) = 252 (100), 318 (57) nm.

(2,6-Dichlorophenyl)-bis(2-pyrrolyl)methane (7)

2,6-Dichlorobenzaldehyde (1.600 g, 9.141 mmol) was dissolved in 50 mL freshly distilled pyrrole and 50 mL TFA were added. The mixture was stirred for 6 h at r.t. and then quenched with 200 mL of CH_2Cl_2 -sat. NaHCO_3 solution (1:1). The organic phase was evaporated and the residue chromatographed on silica (CH_2Cl_2 -hexane, 1:1) under exclusion of light and oxygen to obtain 1.916 g (6.581 mmol, 72%) of **7** as a viscous oil, which crystallized after 24 h at 4 °C.

$R_f = 0.60$ (silica, CH_2Cl_2 -hexane, 1:1).

¹H NMR (300 MHz, CDCl_3): $\delta = 8.27$ (br s, 2 H, HN), 7.34–7.31 (m, 2 H, H-3',5'), 7.15–7.08 (m, 1 H, H-4'), 6.72–6.67 (m, 2 H, H-3,9), 6.48 (br s, 1 H, H-6), 6.20–6.16 (m, 2 H, H-5,7), 6.08–6.04 (m, 2 H, H-4,8).

¹³C NMR (75 MHz, CDCl_3): $\delta = 137.1$ (2 C), 135.9, 129.4 (2 C), 128.7 (2 C), 117.0 (2 C), 108.7 (3 C), 107.4 (2 C), 40.1.

5,15-Bis-(2,6-dichlorophenyl)-10,20-bis(2-benzyloxy)porphyrin (9)

To a solution of dipyrromethane **7** (5.306 g, 18.22 mmol) and benzaldehyde **8** (2.579 g, 12.15 mmol) in 150 mL CH_2Cl_2 , 0.1 mL TFA were added and the solution was stirred at r.t. for 16 h. Subsequently, 3,4,5,6-tetrachloro-1,2-benzoquinone (4 g) were added and the mixture was heated under reflux for 1 h. The solvent was evaporated and the residue chromatographed on silica (CH_2Cl_2) to obtain 1.340 g (1.388 mmol, 22.8%) **9** as a red microcrystalline powder; mp >250 °C.

$R_f = 0.23$ (silica, CH_2Cl_2 -hexane, 1:1).

¹H NMR (300 MHz, CDCl_3): $\delta = 8.84$ (d, $J = 4.8$ Hz, 4 H, pyrrole), 8.65 (d, $J = 4.8$ Hz, 4 H, pyrrole), 8.09–8.05 (m, 2 H, H-4'), 7.83–7.79 (m, 4 H, H-3',5'), 7.78–7.34 (m, 12 H, H-3',5',3'',4'',5'',6''), 6.88–6.60 (m, 10 H, H-2''',3''',4''',5''',6'''), 5.00 (s, 4 H, -O-CH₂-).

MS (LDI-TOF): $m/z = 964.6$.

UV/Vis (CH_2Cl_2): λ_{max} (%) = 418 (100), 514 (8), 586 (5) nm.

The purification of **9** can be improved by preparing the corresponding Zn complex **Zn-9** followed by purification and final Zn removal. For this purpose porphyrin **9** (1.340 g, 1.388 mmol) was dissolved in 100 mL CH_2Cl_2 and after addition of 3 g $\text{Zn}(\text{OAc})_2 \cdot 6\text{H}_2\text{O}$ in 50 mL MeOH the mixture was heated under reflux for 2 h. The organic phase was washed with H_2O , dried over Na_2SO_4 and evaporated yielding a residue which was chromatographed on silica (CH_2Cl_2 -hexane, 1:1); 973.4 mg (946.0 mmol, 68%) **Zn-9** were obtained as a red solid; mp >250 °C.

$R_f = 0.30$ (silica, CH_2Cl_2 -hexane, 1:1).

¹H NMR (300 MHz, CDCl_3): $\delta = 9.0$ (d, $J = 4.8$ Hz, 4 H, pyrrole), 8.8 (d, $J = 4.8$ Hz, 4 H, Pyrrole), 8.2 (m, 2 H, H-4'), 7.9–6.9 (m, 12 H, H-3',5',3'',4'',5'',6''), 6.8–6.4 (m, 10 H, H-2''',3''',4''',5''',6'''), 5.3 (s, 4 H, -O-CH₂-).

UV/Vis (CH_2Cl_2): λ_{max} (%) = 422 (100), 400 (14), 548 (8) nm.

For Zn removal 973.4 mg (946 μmol) **Zn-9** were dissolved in 100 mL CH_2Cl_2 and after addition of 100 mL concd HCl the mixture was stirred for 30 min. The organic phase was neutralized with sat. NaHCO_3 solution, dried over Na_2SO_4 , evaporated and the residue chromatographed on silica (CH_2Cl_2 -hexane, 1:1); 780.6 mg (809 μmol, 86%) of the pure free base porphyrin **9** were isolated as a red solid.

5,15-Bis(2,6-dichlorophenyl)-10,20-bis(2-hydroxyphenyl)porphyrin (αα and αβ 10)

A solution of 780.6 mg (809.1 μmol) porphyrin **9** in 100 mL CHCl_3 was cooled to –78 °C, and then 1.5 mL BBr_3 were added and the solution stirred for 30 min. The reaction was quenched with sat. NaHCO_3 solution and extracted twice with CH_2Cl_2 , the organic phase was dried over Na_2SO_4 , evaporated and the residue chromatographed on silica (CH_2Cl_2) to obtain 268.0 mg (αα) and 338.2 mg (αβ) of **10**; mp >250 °C.

Atropisomerization occurs at 40 °C well below the temperature of the subsequent macrocyclization. Therefore the two isomers were combined for further use.

$R_f = 0.79$ (αα, silica, CH_2Cl_2).

$R_f = 0.25$ (αβ, silica, CH_2Cl_2).

¹H NMR (300 MHz, CDCl_3): $\delta = 8.92$ (m, 4 H, pyrrole), 8.73 (m, 4 H, pyrrole), 8.10–7.20 (m, 14 H, aryl), 5.07 (αα) or 5.02 (αβ) (s, 2 H, OH), –2.55 (s, 2 H, NH).

MS (LDI-TOF): $m/z = 785.3$.

UV/Vis (CH_2Cl_2): λ_{max} (%) = 418 (100), 512 (6) nm.

5,15-([5-(*t*-Butyl)-2-(*N,N*-dimethylcarbamoyl)thio-1,3-phenylene]bis(trimethylenoxy))-di-2,1-phenylene)-10,20-bis(2,6-dichlorophenyl)porphyrin (12)

To a solution of porphyrin **10** (242.4 mg, 308 μ mol) in 150 mL dry DMF 5.5 g Cs₂CO₃ and 40 mg DMAP were added and the mixture stirred for 30 min at 80 °C. Then, dimesylate **11** (157.4 mg, 308 μ mol) in 10 mL DMF was added via automatic syringe during 3 h at 80 °C. Heating was continued for further 1.5 h. The solvent was evaporated, the residue redissolved in CH₂Cl₂, washed with H₂O, dried over Na₂SO₄ and finally chromatographed on silica (CH₂Cl₂) to obtain 270.3 mg (245 μ mol, 79%) of **12** as a purple solid; mp >250 °C.

R_f = 0.16 (silica, CH₂Cl₂).

¹H NMR (300 MHz, CDCl₃): δ = 9.18–8.46 (m, 8 H, pyrrole), 8.76–7.18 (m, 14 H, H-3',4',5',6',3'',4'',5''), 6.64 (s, 2 H, H-3''',5'''), 3.93–3.81 (m, 4 H, H- α'), 2.00–1.50 (br s, 3 H, N-CH₃), 1.48–1.30 (m, 4 H, H- β'), 1.21 (s, 9 H, H-2''''), 1.12–0.93 (m, 4 H, H- γ'), –1.10 to –1.50 (br s, 3 H, N-CH₃), –1.95 (s, 2 H, NH).

¹³C NMR (75 MHz, CDCl₃): δ = 116.3, 159.9, 150.8, 145.2, 139.9, 139.5, 138.8, 138.2, 137.2, 134.0, 130.4, 130.3, 130.0, 129.9, 128.9, 128.1, 128.0, 127.8, 127.5, 127.3, 123.6, 119.5, 116.0, 112.2, 68.7, 34.1, 31.6, 31.0, 30.3.

MS (ESI, MeOH): m/z = 1102.

MS (LDI-TOF): m/z = 1108.0 [M⁺], 1035.5.

UV/Vis (CH₂Cl₂): λ_{\max} (%) = 422 (100), 400 (14), 548 (8) nm.

5,15-([5-(*t*-Butyl)-2-mercapto-1,3-phenylene]bis(trimethylenoxy))-di-2,1-phenylene)-10,20-bis(2,6-dichlorophenyl)porphyrin (13)

To a solution of porphyrin **12** (121.9 mg, 110.6 μ mol) in 15 mL dry oxygen-free dioxane 3.3 mL (11.06 mmol) 25% MeOK solution were added and the solution heated for 2 h at 70 °C. After quenching with 10% HCl solution the mixture was extracted three times with CH₂Cl₂, the organic layer washed with sat. NH₄Cl solution, dried over Na₂SO₄ and evaporated. The residue was chromatographed on silica (CH₂Cl₂–hexane, 1:1) to obtain 53.1 mg (51.51 mmol, 46%) **13** as a red solid; mp >250 °C.

R_f = 0.57 (silica, CH₂Cl₂–hexane, 1:1).

¹H NMR (300 MHz, CDCl₃): δ = 8.90–8.63 (m, 8 H, pyrrole), 7.83–7.18 (m, 14 H, H-3',5',6'), 6.33 (s, 2 H, H-3''',5'''), 3.74 (m, 4 H, CH₂- α'), 1.02 [s, 9 H, C(CH₃)₃''''], 0.95 (m, 4 H, CH₂- β'), 0.67 (m, 4 H, CH₂- γ'), –2.29 (s, 2 H, NH), –2.59 (s, 1 H, SH).

MS (ESI, CH₂Cl₂–MeOH, 1:1): m/z = 1031.4.

MS (LDI TOF): m/z = 1030.3.

UV/Vis (CH₂Cl₂): λ_{\max} (%) = 422 (100), 518 (7) nm.

[5,15-([5-(*t*-Butyl)-mercapto-1,3-phenylene]bis(trimethylenoxy))-di-2,1-phenylene)-10,20-bis(2,6-dichlorophenyl)porphyrinato]iron(III) (14)

In a glove box porphyrin **13** (51 mg, 49.47 μ mol) and approx. 200 mg iron(II)bromide were dissolved in toluene and heated under reflux for 1 h after addition of 20 μ L 2,6-lutidine. The solvent was evaporated and the residue chromatographed on silica (CH₂Cl₂–MeOH, 95:5) to obtain 42.9 mg (39.6 μ mol, 80%) **14** as a brown solid; mp >250 °C.

R_f = 0.30 (silica, CH₂Cl₂–MeOH, 95:5).

HPLC (RP18, hexane–*i*-PrOH, 90:10; flow rate 1.0 mL/min, λ = 410 nm): τ = 12.4 min.

EPR (CDCl₃; T = 121 K) bromide complex: g = 7.45, 4.50, 3.40.

MS (LDI TOF): m/z = 1083.

UV/Vis (CH₂Cl₂): λ_{\max} (%) = 422 (100), 518 (7).

[5,15-([5-(*t*-Butyl)-2-sulfonato-1,3-phenylene]bis(trimethylenoxy))-di-2,1-phenylene)-10,20-bis(2,6-dichlorophenyl)porphyrinato]iron(III) (6)

Bubbling air through a solution of the porphyrin **14** (42.9 mg, 39.6 μ mol) in 10 mL CH₂Cl₂ at r.t. during 15 min gave according to control by UV spectroscopy and MS spectrometry quantitative conversion to **6**.

Compound **6** can also be obtained by iron insertion into the sulfonate corresponding to **13**.

R_f = 0.30 (silica, CH₂Cl₂–MeOH, 95:5).

HPLC (RP18, hexane–*i*-PrOH, 90:10, flow rate 1 mL/min, λ = 410 nm): τ = 12.3 min.

EPR (CDCl₃; T = 121 K): g = 5.76.

MS (LDI TOF): m/z = 1135.

UV/Vis (CH₂Cl₂): λ_{\max} (%) = 414 (100), 512 (9.8) nm.

UV/Vis (THF): λ_{\max} = 416 (100), 510 (17) nm.

5,15-Bis(2-benzyloxy-4-carboxyethylphenylene)-10,20-bis(2,6-dichlorophenyl)porphyrin (17)

To a solution of 2,6-dichlorophenyl dipyrromethane **7** (1.9168 g, 6.583 mmol) and 3-benzyloxy-4-formyl-ethylbenzoate (**16**, 1.5424 g, 6.583 mmol) in 50 mL CH₂Cl₂ 0.5 mL TFA were added and the solution was stirred at r.t. for 2 h. Subsequently, 3 g of 2,3-dichloro-5,6-dicyano-1,4-benzoquinone were added and the mixture stirred for 1 h at r.t. The solvent was largely evaporated at 15 Torr and the residue filtered over silica. The resulting solution was evaporated and subjected to column chromatography on silica (CH₂Cl₂–hexane, 7:3). The porphyrin **17** (722.6 mg, 651.7 μ mol, 20%) was obtained as a red microcrystalline powder; mp >250 °C.

¹H NMR (300 MHz, CDCl₃): δ = 8.88–6.67 (m, 20 H, aryl and pyrrole), 6.90–6.60 (m, 10 H, benzyl), 5.10 (s, 4 H, benzyl-CH₂), 4.58 (q, 4 H, COOCH₂CH₃), 1.55 (t, 6 H, COOCH₂CH₃).

MS (LDI-TOF): m/z = 1109.6.

UV/Vis (CH₂Cl₂): λ_{\max} (%) = 420 (100), 486 (5), 514 (8), 548 (3), 592 (4).

UV/Vis (CH₂Cl₂, HCl): λ_{\max} (%) = 366 (25), 400 (23), 422 (23), 448 (100), 486 (18), 656 (19) nm.

The purification of **17** can be improved by preparing the corresponding Zn complex **Zn-17** followed by purification and final Zn removal. For this purpose porphyrin **17** (400 mg, 360.7 μ mol) was dissolved in 50 mL CH₂Cl₂ and after addition of 2 g Zn(OAc)₂·6H₂O in 5 mL MeOH the mixture was heated under reflux for 1.5 h. The organic phase was washed with H₂O, dried over Na₂SO₄ and evaporated at 15 Torr yielding a residue, which was chromatographed on silica (CH₂Cl₂). After chromatography **Zn-17** (410.1 mg, 350.0 μ mol, 97%) was obtained as a mixture of atropisomers. R_f = 0.52 ($\alpha\alpha$) und 0.60 ($\alpha\beta$) (silica, CH₂Cl₂–hexane, 80:20). Mp >250 °C.

UV/Vis (CH₂Cl₂): λ_{\max} (%) = 422 (100), 496 (14), 552 (11) nm.

For Zn removal **Zn-17** (410.1 mg, 350.0 μ mol) was dissolved in 20 mL CH₂Cl₂ and after addition of 5 mL concd HCl the mixture was stirred for 1 h. The green solution was diluted with 50 mL H₂O, and washed with 100 mL sat. NaHCO₃ solution NaHCO₃. The resulting red solution was evaporated and the residue chromatographed on silica (CH₂Cl₂–hexane, 7:3); 376.3 mg (339.3 μ mol, 97%) of the pure free base porphyrin **17** were isolated.

5,15-Bis(4-carboxyethyl-2-hydroxyphenyl)-10,20-bis(2,6-dichlorophenyl)porphyrin (18)

A solution of porphyrin **17** (187.2 mg, 169.2 μ mol) in 30 mL abs. CH₂Cl₂ was cooled to –78 °C (acetone/CO₂), BBr₃ (0.3 mL) was added and the green solution stirred for 1 h. The reaction was

quenched with 100 mL H₂O, the organic layer washed with sat. NaHCO₃ and dried over Na₂SO₄. Finally, the product was purified on silica (CH₂Cl₂-MeOH, 97:3) yielding 134.3 mg (145 mmol, 86%) red, microcrystalline **18**; mp >250 °C.

$R_f = 0.4$ ($\alpha\beta$) and 0.6 ($\alpha\alpha$) (silica, CH₂Cl₂-MeOH, 97:3).

¹H NMR (300 MHz, CDCl₃): $\delta = 8.79-7.22$ (m, 20 H, aryl and pyrrol), 4.46 (q, 4 H, COOCH₂CH₃), 1.47 (t, 6 H, COOCH₂CH₃), -1.20 (2 s, 2 H, NH).

MS (LDI-TOF): $m/z = 932.6$.

UV/Vis (CH₂Cl₂): $\lambda_{\max} (\%) = 418$ (100), 512 (6) nm.

5,15-Bis(4-carboxyethyl)-{[5-(*tert*-butyl)-2-*N,N*-dimethyl-carbamoyl]-thio-1,3-phenylene}-bis-[(trimethyleneoxy)di-2,1-phenylene]-10,20-bis-(2,6-dichlorophenyl)porphyrin (19**)**

To a solution of porphyrin **18** (134.3 mg, 145 mmol) in 70 mL dry DMF (degassed) 2.0 g Cs₂CO₃ and 20 mg DMAP were added and the mixture heated at 80 °C for 30 min. The dimesylate **11** (81.3 mg, 159 mmol) dissolved in 5 mL DMF was subsequently added via automatic syringe during 3 h at 80 °C. Heating was continued for further 1.5 h. After evaporation of DMF the residue was dissolved in CH₂Cl₂, washed with H₂O, dried over Na₂SO₄ and finally chromatographed on silica (CH₂Cl₂-MeOH, 99:1). The mono-bridged porphyrin **19** (152.29 mg, 122 mmol) was obtained as a red microcrystalline substance in 84% yield; mp >250 °C.

$R_f = 0.5$ (silica, CH₂Cl₂-MeOH, 99:1).

IR (KBr): 3500 (br), 2928.9 (m), 1717.3 (s), 1427.7 (m), 1285.6 (s), 1102.8 (m), 801.4 (m) cm⁻¹.

¹H NMR (300 MHz, CDCl₃): $\delta = 9.11-7.55$ [m, 20 H, H- β (pyrrol) and H-3', H-4', H-5', H-6', H-3'', H-4'', H-5''], 6.64 (s, 2 H, H-3''', H-5'''), 4.63 (q, 4 H, COOCH₂CH₃), 4.01, 3.90 [m, 6 H, N(CH₃)₂], 1.60 (t, 6 H, COOCH₂CH₃), 1.37 (br, 4 H, H- α'), 1.20 [s, 9 H, (CH₃)₃], 1.00 (br, 4 H, H- β'), 0.79 (br, 4 H, H- γ'), -1.34 (br, 2 H, NH).

¹³C NMR (75 MHz, CDCl₃): $\delta = 166.8, 166.4, 160.0, 151.2, 145.3, 140.0, 139.4, 139.3, 138.9, 138.3, 137.3, 135.3, 134.0, 132.4, 130.6, 130.2, 128.2, 128.1, 127.9, 127.8, 127.5, 123.9, 123.8, 121.1, 115.2, 113.0, 69.1, 61.5, 34.3, 31.7, 31.3, 31.2, 30.9, 30.2, 14.7, 14.6$.

MS (ESI, MeCN): $m/z = 1246.5$.

MS (LDI-TOF): $m/z = 1247.6$.

UV/Vis (CH₂Cl₂): $\lambda_{\max} (\%) = 422$ (100), 516 (6), 548 (3), 592 (2) nm.

5,15-Bis(4-carboxyl-){[5-(*tert*-butyl)-2-mercapto-1,3-phenylene]-bis(trimethyleneoxy)}di-2,1-phenylene)-10,20-bis(2,6-dichlorophenyl)porphyrin (20**)**

The porphyrin **19** (143.0 mg, 114.7 mmol) was dissolved in 20 mL dry oxygen-free dioxane. After addition of 3.5 mL 25% MeOK-MeOH the mixture was heated for 2.5 h at 65 °C. The reaction was quenched with 50 mL 10% HCl and extracted three times with 50 mL CH₂Cl₂. The organic layer was washed with sat. aq NH₄Cl and dried over Na₂SO₄. Chromatography on silica (CH₂Cl₂-MeOH-HOAc, 96:3:1) furnished the diacid **20** (111.9 mg, 100 mmol) in 87% yield; mp >250 °C.

$R_f = 0.4$ (silica, CH₂Cl₂-MeOH-HOAc, 96:3:1).

IR (KBr): 3440.2 (br), 2923.9 (m), 1683.8 (s), 1591.1 (m), 1364.4 (m), 800.8 (w), 764.1 (m), 698.7 (w) cm⁻¹.

¹H NMR (300 MHz, CDCl₃ with CD₃COOD): $\delta = 8.83-7.67$ [m, 20 H, H- β (pyrrol), H-3', H-4', H-5', H-6', H-3'', H-4'', H-5''], 6.59 (s, 2 H, H-3''', H-5'''), 1.30 (br, 4 H, H- α'), 1.01 [s, 9 H, (CH₃)₃], 0.92 (br, 4 H, H- β'), 0.69 (br, 4 H, H- γ'), -2.32 (s, 2 H, NH), -2.64 (s, 1 H, SH).

MS (ESI, MeCN): $m/z = 1119.5$.

UV/Vis (CH₂Cl₂): $\lambda_{\max} (\%) = 302$ (9), 422 (100), 516 (9), 548 (3), 592 (3) nm.

[5,15-Bis(4-carboxyl-){[5-(*tert*-butyl)-2-mercapto-1,3-phenylene]bis(trimethyleneoxy)}di-2,1-phenylene]-10,20-bis(2,6-dichlorophenyl)porphyrinato]iron(III) (21**)**

In a glove box (<20 ppm O₂) porphyrin **20** (111.9 mg, 100 mmol) were dissolved in 20 mL DMF and after addition of 50 μ L 2,6-lutidine and 300 mg iron(II)bromide the mixture was heated to 160 °C for 3 h. DMF was evaporated and the residue purified on silica (CH₂Cl₂-MeOH-HOAc, 96:3:1). The iron(III) complex **21** was isolated as a brown solid (71.3 mg, 60.8 mmol) in 61% yield.

$R_f = 0.3$ (silica, CH₂Cl₂-MeOH-HOAc, 96:3:1).

Mp >250 °C.

MS (ESI): $m/z = 1168.1$.

UV/Vis (CH₂Cl₂): $\lambda_{\max} (\%) = 338$ (20), 422 (100), 514 (8) nm.

UV/Vis (MeOH): $\lambda_{\max} (\%) = 422$ (50.8), 518 (4.6), 548 (1.9), 592 (1.9) nm.

Tentagel-linked Fe-OSO₂ porphyrin (15**)**

A solution of iron porphyrin **21** (9.0 mg, 7.680 mmol) in 5 mL DMF was aired for 15 min and the complete oxidation at sulfur controlled by UV/Vis ($\lambda_{\max} = 415$ nm) and by ESI-MS spectrometry ($m/z = 1220.2$). Subsequently, 201.1 mg RAPP Tentagel-S-NH₂, 0.3 mL DCC and 2 mL CH₂Cl₂ were added. The mixture was stirred for 12 h at r.t. and finally the polymer collected by filtration and washed with CH₂Cl₂, MeOH, DMF and HOAc (5 mL each). The volume of the combined filtrates was adjusted to 200 mL, and from UV absorbance an epitopic density on the gel was calculated 18.1 mmol/g RAPP Tentagel. This value was confirmed through re-isolation of the uncoupled **21** from the filtrate.

Then, 30 mg of **15** was suspended in CH₂Cl₂ and the unmodified amino groups acetylated with an excess of HOAc and DCC; the resulting sample was negative in a ninhydrin test. The polyacetylated gel was then reacted with an excess of 1,2 diamino ethane and DCC in order to derivatize the free COOH groups at the porphyrin. Quantitative analysis of the Ninhydrin test revealed an epitopic density of 22 mmol/g.

The good agreement of the two values of the epitopic density indicates the absence of cross-linking of **21** with the RAPP Tentagel.

General Procedure for Epoxidations

In a 20 mL Schlenk-tube the substrate, PhIO, porphyrin **6** (RAPP-porphyrin **15**), and decane (internal standard) were dissolved in 5 mL CH₂Cl₂. Concentrations: catalysts: <0.1 mol%, olefin: 0.5 mmol, PhIO: 1 mmol; reaction time 24 h at r.t. The reaction was controlled by GC-FID and the turnover was quantified in reference to the internal standard.

Acknowledgment

WDW gratefully acknowledges financial support by the Swiss National Foundation.

References

- (1) Ortiz de Montellano, P. R. *Cytochrome P450 Structure, Mechanism and Biochemistry*; Plenum Press: New York, London, **1986**.
- (2) Omura, T.; Sato, R. *J. Biol. Chem.* **1964**, 239, 2370.
- (3) Woggon, W.-D. *Top. Curr. Chem.* **1997**, 184, 39.

- (4) (a) Stäubli, B.; Fretz, H.; Piantini, U.; Woggon, W.-D. *Helv. Chim. Acta* **1987**, *70*, 1173. (b) Aissaoui, H.; Ghirlanda, S. L.; Gmür, C.; Woggon, W.-D. *J. Mol. Catal.* **1996**, *113*, 393. (c) Aissaoui, H.; Bachmann, R.; Schweiger, A.; Woggon, W.-D. *Angew. Chem. Int. Ed.* **1998**, *37*, 2998.
- (5) Patzelt, H.; Woggon, W.-D. *Helv. Chim. Acta* **1992**, *75*, 523.
- (6) Woggon, W.-D. *Chimia* **2001**, *55*, 366.
- (7) Sligar, S. G.; Gunsalus, I. C. A. *Proc. Natl. Acad. Sci. U.S.A.* **1976**, *73*, 1078.
- (8) Poulos, T. L. *J. Biol. Inorg. Chem.* **1996**, *1*, 356.
- (9) Ueyama, N.; Nishikawa, N.; Yamada, Y.; Okamura, T.-A.; Nakamura, A. *J. Am. Chem. Soc.* **1996**, *118*, 12826.
- (10) De Visser, S. P.; Ogliaro, F.; Sharma, P. K.; Shaik, S. *J. Am. Chem. Soc.* **2002**, *124*, 11809.
- (11) (a) Ogliaro, F.; Cohen, S.; de Visser, S. P.; Shaik, S. *J. Am. Chem. Soc.* **2000**, *122*, 12892. (b) Schöneboom, J. C.; Lin, H.; Reuter, N.; Thiel, W.; Cohen, S.; Ogliaro, F.; Shaik, S. *J. Am. Chem. Soc.* **2002**, *124*, 8142.
- (12) Shaik, S.; de Visser, S. P.; Ogliaro, F.; Schwarz, H.; Schröder, D. *Curr. Opin. Chem. Biol.* **2002**, *6*, 556.
- (13) Shaik, S.; Cohen, S.; de Visser, S. P.; Sharma, P. K.; Kumar, D.; Kozuch, S.; Ogliaro, F.; Danovich, D. *Eur. J. Inorg. Chem.* **2004**, *35*, 207.
- (14) *Jaguar 4.2*; Schrödinger, Inc.: Portland, OR, **2000**.
- (15) Frisch, M. J.; Trucks, G. W.; Schlegel, H. B.; Scuseria, G. E.; Robb, M. A.; Cheeseman, J. R.; Zakrzewski, V. G.; Montgomery, J. A. Jr.; Stratmann, R. E.; Burant, J. C.; Dapprich, S.; Millam, J. M.; Daniels, A. D.; Kudin, K. N.; Strain, M. C.; Farkas, O.; Tomasi, J.; Barone, V.; Cossi, M.; Cammi, R.; Mennucci, B.; Pomelli, C.; Adamo, C.; Clifford, S.; Ochterski, J.; Petersson, G. A.; Ayala, P. Y.; Cui, Q.; Morokuma, K.; Malick, D. K.; Rabuck, A. D.; Raghavachari, K.; Foresman, J. B.; Cioslowski, J.; Ortiz, J. V.; Baboul, A. G.; Stefanov, B. B.; Liu, G.; Liashenko, A.; Piskorz, P.; Komaromi, I.; Gomperts, R.; Martin, R. L.; Fox, D. J.; Keith, T.; Al-Laham, M. A.; Peng, C. Y.; Nanayakkara, A.; Gonzalez, C.; Challacombe, M.; Gill, P. M. W.; Johnson, B. G.; Chen, W.; Wong, M. W.; Andres, J. L.; Head-Gordon, M.; Replogle, E. S.; Pople, J. A. *Gaussian, Inc.: Pittsburgh, PA*, **1998**.